Supplementary Figures

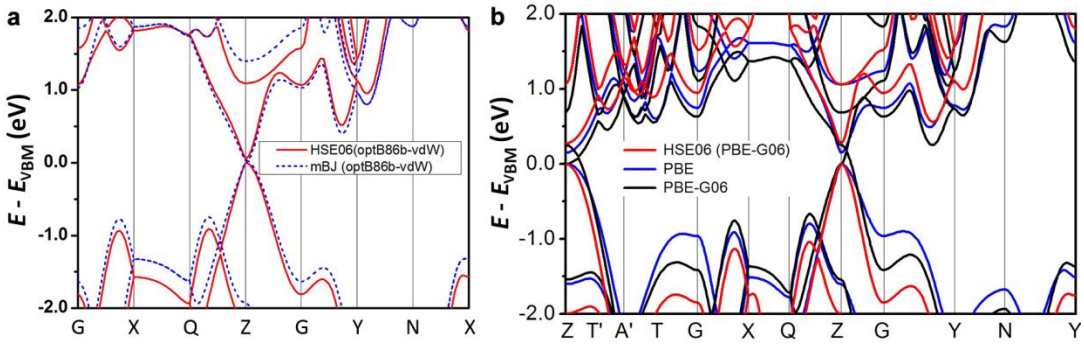

Supplementary Figure 1 | Electronic bandstructures of bulk BP calculated with different functionals. **a,** HSE06[1, 2] (red solid lines) and LDA-mBJ[3, 4] (blue dashed lines) bandstructures based on the atomic structure optimized by optB86b-vdW[5, 6], denoted mBJ (optB86b-vdW) and HSE06 (optB86b-vdW). **b,** Bandstructures calculated with HSE06 (PBE-G06[7, 8]) (red), PBE[7] (blue) and PBE-G06 (black).

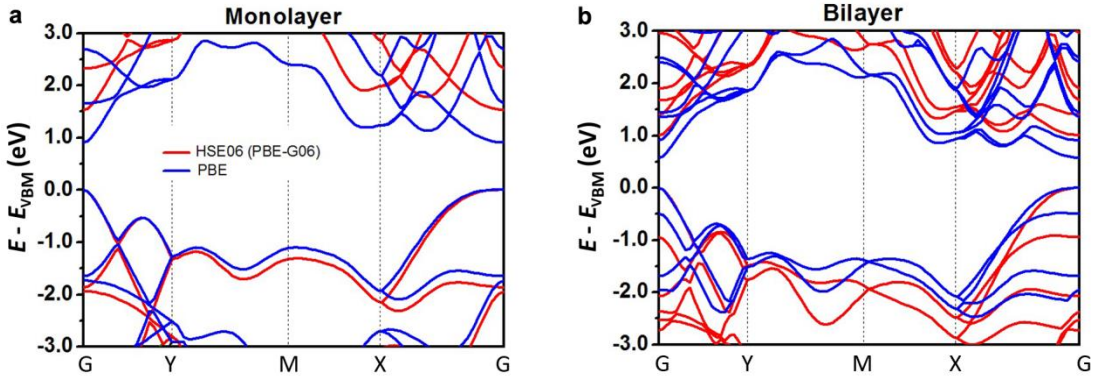

Supplementary Figure 2 | Electronic bandstructures of monolayer, a, and bilayer, b, BP. Results were obtained using the HSE06 functional based on the atomic structure from PBE-G06 (red) and PBE functional (blue).

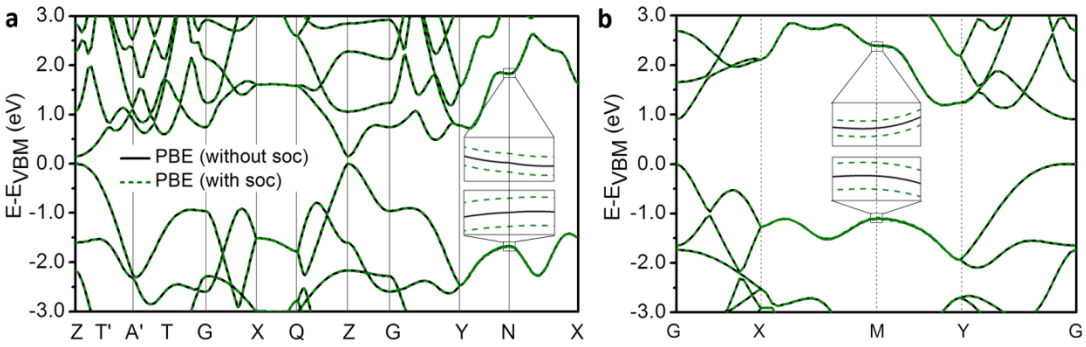

Supplementary Figure 3 | Electronic bandstructures of bulk, a, and monolayer, b, BP, calculated by PBE with (green dashed lines) and without (black solid lines) SOC. Insets provide a magnification to show SOC effects around the N (M) point.

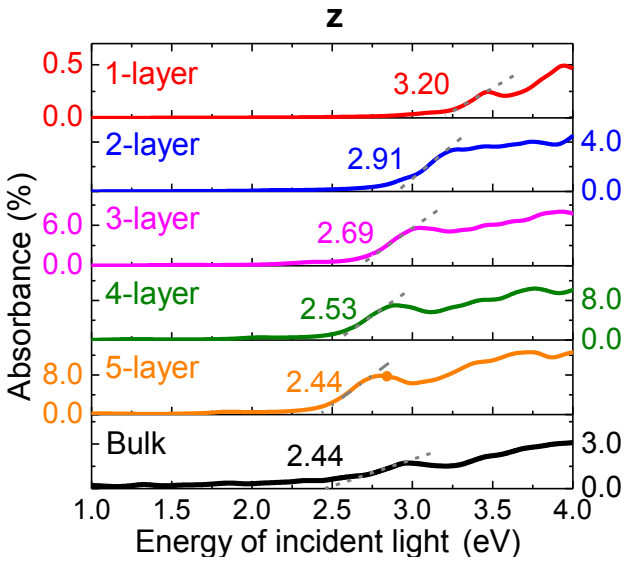

Supplementary Figure 4 | Theoretically predicted optical absorption spectra of few-layer BP systems for light incident along an in-plane direction and polarized in *c (z)* direction. Black dashed lines indicate the linear fit used to estimate the absorption edge. No appreciable absorption is found for energies below 2.0 eV. As for the case of *y*-polarized light shown in Fig. 3**b**, the bandgap process is symmetry-forbidden and absorption processes begin only beyond 2 eV. Thus the absorption exhibits an explicit anisotropy for light polarized in all three polarization directions. This behaviour should be readily detectable in spectroscopic measurements and may be exploited for optoelectronic applications.

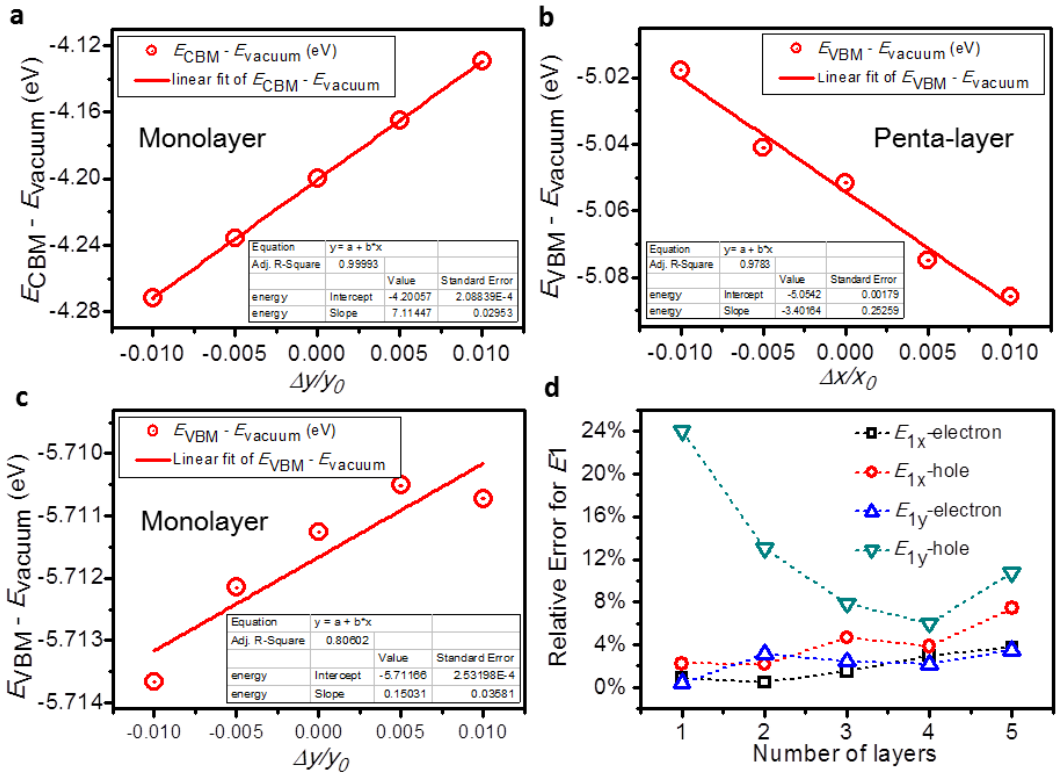

Supplementary Figure 5 | Relative error in the deformation potential. Band energy of the CBM of monolayer BP **a** and of the VBMs of 5-layer, **b,** and monolayer, **c,** BP with respect to the vacuum energy as a function of lattice dilation. Band energies were calculated with the HSE06 functional. Red solid lines are the fitting curves. Insets show the standard errors of the fitted slope, which corresponds to the deformation potential. All relative errors for the deformation potential of few-layer BP for the *x* and *y* directions are summarized in panel **d**.

Supplementary Tables

Supplementary Table 1 | Lattice constants and structural parameters of bulk black phosphorus calculated using different computational methods.

Functional	a (Å)	b (Å)	c (Å)	$R1$ (Å)	$R2$ (Å)	$\theta 1$ (°)	$\theta 2$ (°)
Expt.[9]	4.38	3.31	10.48	2.24	2.22	102.09	96.34
PBE	4.57	3.30	11.33	2.26	2.22	103.59	95.98
PBE[10]	4.54	3.28	11.22	-	-	-	-
PBE-G06	4.43	3.32	10.49	2.26	2.23	102.48	96.50
PBE-G06[10]	4.40	3.30	10.43	-	-	-	-
PBE-TS[10]	4.39	3.29	10.82	-	-	-	-
RPBE-G06	4.57	3.33	10.91	2.27	2.23	103.58	96.42
HSE06-G06	4.42	3.30	10.43	2.23	2.20	102.87	96.96
optPBE-vdW	4.54	3.34	10.95	2.28	2.24	103.02	96.07
optB86b-vdW	4.35	3.33	10.52	2.27	2.24	101.58	96.09
optB88-vdW	4.47	3.34	10.71	2.28	2.25	102.42	96.16
PW91 (S1)	4.55	3.31	11.18	2.27	2.23	103.45	96.04
PW91 (S2)	4.56	3.31	11.19	2.27	2.23	103.46	96.03
PW91-G06	4.43	3.33	10.48	2.27	2.23	102.47	96.57
PW91[11]	4.42	3.35	10.59	2.26	2.24	102.31	96.85

The functionals adopted are PBE, RPBE[12] and HSE06 and the dispersion forces are taken into account at the DFT-G06[8] and vdW-DF[13] levels.

Supplementary Table 2 | Bandgaps of few-layer BP.				
Number of Layers	HSE06 (optB88-vdW)	mBJ (optB88-vdW)	HSE06 (PBE-G06)	PBE (PBE)
1	1.51	1.41	1.53	0.91
2	1.02	0.94	1.01	0.58
3	0.79	0.72	0.73	0.42
4	0.67	0.61	0.61	0.36
5	0.59	0.54	0.52	0.28
∞	0.53	0.49	0.45	0.24
Bulk	0.36	0.31	0.27	0.15
Exact values, in units of eV, of bandgaps plotted in Fig. 2**h** and Supplementary Fig. 2.				

Supplementary Table 3 | Carrier mobility predicted by the 1D model.

Carrier type	N_L	m_x^*/m_0 G-X	m_y^*/m_0 G-Y	E_{1x} (eV)	E_{1y} (eV)	C_{x_1D} (10^{-7} J m^{-1})	C_{y_1D} (10^{-7} J m^{-1})	μ_{x_1D} (10^3cm^2 V^{-1} s^{-1})	μ_{y_1D} (10^3cm^2 V^{-1} s^{-1})
e	1	0.17	1.12	2.72±0.02	7.11±0.02	2.90	10.16	5.4-5.6	~0.24
	2	0.18	1.13	5.02±0.02	7.35±0.16	5.74	19.46	~3.0	0.38-0.44
	3	0.16	1.15	5.85±0.09	7.63±0.18	8.58	28.72	3.8-4.0	0.52-0.58
	4	0.16	1.16	5.92±0.18	7.58±0.13	11.46	37.94	4.8-5.4	0.70-0.76
	5	0.15	1.18	5.79±0.22	7.35±0.26	14.66	47.98	6.8-8.0	0.88-1.0
h	1	0.15	6.35	2.50±0.06	0.15±0.03	2.90	10.16	7.6-8.2	26-66
	2	0.15	1.81	2.45±0.05	1.63±0.16	5.74	19.46	16-17	3.2-5.4
	3	0.15	1.12	2.49±0.12	2.24±0.18	8.58	28.72	22-26	5.6-7.8
	4	0.14	0.97	3.16±0.12	2.79±0.13	11.46	37.94	20 -24	6.2-7.8
	5	0.14	0.89	3.40±0.25	2.97±0.18	14.66	47.98	20-28	7.2-11

E_{1x} (E_{1y}) and C_{x_1D} (C_{y_1D}) are the deformation potential and effective elastic modulus of a 10 nm BP ribbon for the x (y) direction. Mobilities μ_{x_1D} and μ_{y_1D} were calculated using Supplementary Equation (2).

Supplementary Discussion

Predicted carrier mobility of few-layer BP with other models

Because the anisotropies of the carrier mobilities are crucial in determining the physical properties of few-layer BP systems, we discuss this issue in more detail here. First, an alternative expression for the mobility which can be found in a number of studies of anisotropic 2D systems is [14-17]

$$\mu_{x\_2D\_AS} = \frac{2e\hbar^3 C_{x\_2D}}{3k_B T (m_e^*)^2 E_{1x}^2} \quad (1)$$

where m_e^* is the effective mass along the transport direction and T is the temperature. We believe that this model, which contains no effective connection between the perpendicular directions, overestimates the extent of anisotropy and therefore we do not consider it further here. An expression for the mobility in 1D systems is [18]

$$\mu_{x\_1D} = \sqrt{\frac{2}{\pi}} \frac{e\hbar^2 C_{x\_1D}}{(k_B T)^{1/2} (m_e^*)^{3/2} E_{1x}^2} \quad (2)$$

which should be relevant for BP ribbons. The narrower the ribbon, the smaller is its effective elastic modulus, and in Supplementary Table 3 we present mobility values calculated from Supplementary Eq. (2) for BP ribbons of 10nm in width, which is a reasonable value for experimental fabrication. Our results show that the 1D mobilities are rather large compared with the values obtained in the 2D model used in the main text. Thus we suggest that etching a 2D BP sheet to produce a 1D ribbon could enhance the carrier mobilities quite significantly, although we caution that the edge structure and its role in electron scattering require further investigation.

Supplementary Methods

Best-fit functionals for few-layer black phosphorus

Supplementary Figure 1 shows that methods HSE06-G06[1, 2, 8], PBE-G06[7, 8] and optB86b-vdW[5] reproduce very accurately the experimental geometry and the theoretical equilibrium volumes are respectively just 0.1% smaller, 1% larger and 0.1% larger than the experiment.[9, 19] The results using PBE[7] and PBE-G06 are consistent with a previous study[10]. In calculations for the exchange-correlation energy performed with PW91[20], we used two approaches to find the equilibrium crystal structure of bulk BP. The results from these two schemes are consistent with each other and, as expected, similar to those of PBE, but differ significantly from the PW91 results of one other study.[11] However, our PW91-G06 results do appear similar to the ``PW91" results of that work [11]. The functional optB88-vdW[5, 6] provides the second best results in terms of geometry, yielding an equilibrium volume only 5% larger than the experiment. The calculated bond lengths are similar for all methods other than HSE06-G06, which predicts bond lengths considerably smaller than any of the others.

Although the geometry is very accurately reproduced by optB86b-vdW, the associated bandgaps are only 0.03 eV (mBJ) and 0.05 eV (HSE06). Similarly small gaps are obtained in the mBJ and HSE06 bandstructures based on the PBE-G06 or HSE06-G06 geometries. The PBE-G06 bandstructure even reports a negative band gap. Thus we conclude that the combinations of mBJ and HSE06 functionals with the PBE-G06, HSE06-G06 and optB86b-vdW schemes are not acceptable for predicting the electronic structure of few-layer BP. In addition, BP appears to be metallic, with a band crossing near the Z point in the PBE-G06 bandstructure; by contrast, in the PBE bandstructure one finds a direct gap of 0.15 eV, a result we ascribe to the fact that PBE overestimates the unit-cell volume, giving rise to a smaller overlap, a weaker interaction and thus a larger gap than that obtained by PBE-G06. The combination of HSE06 or mBJ with the optB88-vdW structure thus provides the best prediction for BP, offering the second-best geometry and the best electronic bandstructure

Supplementary References

1. Heyd, J., Scuseria, G. E. & Ernzerhof, M. Hybrid functionals based on a screened Coulomb potential. *J. Chem. Phys.* **118**, 8207 (2003).

2. Heyd, J., Scuseria, G. E. & Ernzerhof, M. Erratum: "Hybrid functionals based on a screened Coulomb potential" [J. Chem. Phys. 118, 8207 (2003)]. *J. Chem. Phys.* **124**, 219906 (2006).

3. Becke, A. D. & Johnson, E. R. A simple effective potential for exchange. *J. Chem. Phys.* **124**, 221101 (2006).

4. Tran, F. & Blaha, P. Accurate band gaps of semiconductors and insulators with a semilocal exchange-correlation potential. *Phys. Rev. Lett.* **102**, 226401 (2009).

5. Klimeš, J., Bowler, D. R. & Michaelides, A. Van der Waals density functionals applied to solids. *Phys. Rev. B* **83**, 195131 (2011).

6. Klimes, J., Bowler, D. R. & Michaelides, A. Chemical accuracy for the van der Waals density functional. *Condens. Matter Phys.* **22**, 022201 (2010).

7. Perdew, J. P., Burke, K. & Ernzerhof, M. Generalized Gradient Approximation Made Simple. *Phy. Rev. Lett.* **77**, 3865-3868 (1996).

8. Grimme, S. Semiempirical GGA-type density functional constructed with a long-range dispersion correction. *J. Comput. Chem.* **27**, 1787-1799 (2006).

9. Brown, A. & Rundqvist, S. Refinement of the crystal structure of black phosphorus. *Acta Cryst.* **19**, 684-685 (1965).

10. Appalakondaiah, S. *et al.* Effect of van der Waals interactions on the structural and elastic properties of black phosphorus. *Phys. Rev. B* **86**, 035105 (2012).

11. Du, Y., Ouyang, C., Shi, S. & Lei, M. Ab initio studies on atomic and electronic structures of black phosphorus. *J. Appl. Phys.* **107**, 093718 (2010).

12. Hammer, B., Hansen, L. B. & Nørskov, J. K. Improved adsorption energetics within density-functional theory using revised Perdew-Burke-Ernzerhof functionals. *Physical Review B* **59**, 7413-7421 (1999).

13. Dion, M. *et al.* Van der Waals density functional for general geometries. *Phys. Rev. Lett.* **92**, 246401 (2004).

14. Northrup, J. Two-dimensional deformation potential model of mobility in small molecule organic semiconductors. *Appl. Phys. Lett.* **99**, 062111 (2011).

15. Takagi, S.-I., Hoyt, J. L., Welser, J. J. & Gibbons, J. F. Comparative study of phonon-limited mobility of two-dimensional electrons in strained and unstrained Si metal-oxide-semiconductor field-effect transistors. *J. Appl. Phys.* **80**, 1567-1577 (1996).

16. Walukiewicz, W., Ruda, H., Lagowski, J. & Gatos, H. Electron mobility in modulation-doped heterostructures. *Phys. Rev. B* **30**, 4571-4582 (1984).

17. Price, P. Two-dimensional electron transport in semiconductor layers. I. Phonon scattering. *Ann. Phys.* **133**, 217-239 (1981).

18. Beleznay, F., Bogar, F. & Ladik, J. Charge carrier mobility in quasi-one-dimensional systems: Application to a guanine stack. *J. Chem. Phys.* **119**, 5690-5695 (2003).

19. Hultgren, R., Gingrich, N. S. & Warren, B. E. The atomic distribution in red and black phosphorus and the crystal structure of black phosphorus. *J. Chem. Phys.* **3**, 351 (1935).

20. Perdew, J. P. *et al.* Atoms, molecules, solids, and surfaces: Applications of the generalized gradient approximation for exchange and correlation. *Physical Review B* **46**, 6671-6687 (1992).